18th Brazilian Congress of Thermal Sciences and Engineering
November 16–20, 2020 (online)

ENC-2020-0071
COMPARATIVE STUDY OF GEOTHERMAL AND CONVENTIONAL AIR CONDITIONER: A CASE OF STUDY FOR OFFICE APPLICATIONS

Willian Moreira Duarte
Federal University of Minas Gerais (UFMG), Graduate Program in Mechanical Engineering, Belo Horizonte - MG, Brazil
University Center of Belo Horizonte (UniBH), Department of Mechanical Engineering, Av. Prof. Mário Werneck, 1685, Estoril, 30575-180, Belo Horizonte (MG), Brazil
willianmoreiraduarte@gmail.com

Tiago de Freitas Paulino
Federal Center of Technological Education of Minas Gerais (CEFET-MG), Department of Materials Engineering, Av. Amazonas, 5253, Nova Suiça, 30421-169, Belo Horizonte (MG), Brazil
tfpaulinoeng@gmail.com

Sinthya Gonçalves Tavares
André Gonçalves de Oliveira
Luiz Machado
Federal University of Minas Gerais (UFMG), Department of Mechanical Engineering, Av. Antonio Carlos, 6627, Belo Horizonte - MG, 31270-901, Brazil
tavaressinthya@gmail.com, andreqix@hotmail.com, luizm@demec.ufmg.br

Abstract. *The high cost of electricity has done that the air condition sector search for alternatives to produce cold efficiently. It is a necessity, especially in Brazil, where 17% of the total electricity consume is due air condition systems. Many studies have presented technical-economic data of heat-pumping and air conditioner systems but there is a lack of studies that consider applications with only cooling demand. This work presents a comparative analysis of conventional and a ground source air conditioning system. The geothermal air conditioner used an open loop water. The systems are design and simulated for cooling an office considering the climate of Belo Horizonte, Brazil using weather data obtained from June of 2019 to May of 2020. The refrigerant and expansion device chosen was the R410A and capillary tube due availability of commercial components. In order to evaluate the performance of the geothermal and conventional air conditioner a quasi-steady-state model was developed using the Equation Engineering Solver (EES). The results are presented for twelve different scenarios based in three water well temperatures and four water well depth. In the best scenario, the geothermal system has annual energy consumption 33% lower than convention system and a payback time of 1.7 years.*

Keywords: *Geothermal, HVAC, Mathematical model, Payback*

1. INTRODUCTION

The currently goal in air conditioning sector are to produce cold efficiently and if possible off-peak times. It occurs because of the high electricity consumption in the air conditioning sector. In 2017, the air conditioning system electricity consume represents 17% of the total electricity consume in in Brazilian residences (EPE, 2018). Furthermore, air conditioning systems consumes 40.3% of electricity in commercial sector (PROCEL, 2008). In addition, there is a study using world data that informed that the air conditioning systems accounts for 85% of consumption of residential electricity at the peak of summer (Li *et al.*, 2019).

In an attempt to find a technical and economical solution for air conditioners for small environments such as home Petit and Meyer (1997) carried out a comparison of economic viability in South Africa between horizontal-ground-source and air-source systems. The researches concluded that the COP values for heating and cooling of ground-source systems are higher than air-source systems by 30 to 70%. However the cost of installation of air-source systems are cheaper than ground-source, but the cost of operating ground-source is lower. It also concludes that ground-source systems are more viable compared to air-source systems.

Yu *et al.* (2014) presented a systematic study of a coupled geothermal cooling system with an earth-to-air heat exchanger and a solar collector enhanced solar chimney. Three different tests were carried out during 43 days in sequence in the summer. They were started from a passive cooling mode to an active cooling mode, and then back to a passive cooling mode. The authors concluded that geothermal system is feasible to provide cooling to the facility in natural operation mode free without using any electricity. They also concluded that underground heat dissipates faster in the horizontal level than vertical level and the surrounding soil of the earth tube may saturate and takes long to recover if the heat is over-extracted from the soil in a forced air mode.

Kharseh *et al.* (2015) presented an investigation of alternative renewable energy option for reducing energy consumption of air conditioning systems in the residential buildings located in Doha, Qatar. The authors compared two types of air conditioning systems, the conventional system and the ground source heat pump (GSHP). The results presented in the paper demonstrates the energy savings by using GSHP systems due high thermal performance, GSHP is considered a viable solution for reducing energy consumption of heating and air conditioning systems. The payback time of the proposed system is 9 year.

Beckers *et al.* (2018) investigated techno-economic performance of hybrid ground-source heat pump systems for cooling-dominated applications. This system provided an average cooling load of 11 kW for a cellular tower shelter installed in the city of Varna, New York. The paper presented five cases for cellular tower shelter cooling, simulated with TRNSYS. In case 1, all shelter cooling is provided with GSHP. In case 2, GSHP and air economizer. In case 3, GSHP and dry cooler. Case 4, air source heat pump (ASHP). Case 5, ASHP and air economizer. The author concluded with the simulation that the case 5 had the lowest total cost for the ownership. The case 2 had the lowest energy consumption and the case 4 had the highest consumption. They also concluded that simulations indicate that for the Varna Site weather and operational conditions, ground source heat pump-based systems allow the owner to save up to 30% of lifetime electricity consumption in comparison with air-source heat pump-based systems.

Most of papers found in the literature presents a study in application with cooling and heating demand, but none study considered applications with only cooling demand. This work presents a comparative analysis of conventional air conditioner system and a ground source air conditioning system. The Geothermal air conditioner uses an open loop water. The systems are design for cooling an office considering the climate of Belo Horizonte (MG), Brazil.

2. METHODOLOGY

The two system considered in this study are shown in Fig. 1. In the conventional system the main components are the hermetic reciprocating compressor, two cross flow unmixed air-cooled heat exchanger and a capillary tube. The data used in the model are based in the air conditioner model HAFE09B2 manufactured by Elgin. The main difference of the conventional system and geothermal system is the coaxial water-cooled condenser that is cooled by water pumped from a water well. The use of water well in similar device is presented by Blázquez *et al.* (2020). An important step of this work is the economic analysis, therefore the refrigerant chosen is the R410A due availability of commercial components although there is studies (Tian *et al.*, 2015) to replace the use R410A in this type of device due the its high impact in global warming.

2.1 Air conditioner mathematical model

In order to evaluate the performance of the geothermal and conventional air conditioner a quasi-steady-state model was developed using the Equation Engineering Solver (EES). The losses in the tubes between components was considered negligible. The evaporator and condenser was assumed as isobaric and a lumped model was used. Following is described the modelling equation for each component.

2.1.1 Compressor model

The hermetic compressor selected for this work is the model HGA5494BXD manufactured by Tecumseh. In the literature, there are detailed model of compressor (Duprez *et al.*, 2007; Ndiaye and Bernier, 2010; Duarte *et al.*, 2019b) but these models required many parameters and geometrical details that are not provide by the manufactures of hermetic compressors. Additionally, the compressor model used in the complete model of the refrigeration system is a simple one, assuming a isentropic compression process, as those employed in other works (Minetto, 2011; Rabelo *et al.*, 2019; de Paula *et al.*, 2020). The manufacturer of the compressor presents the following equation to evaluate the R410A mass flow rate ($\dot{m}$) and the electric input power ($\dot{W}_{cp}$) in function of the evaporation temperature (T_e) and condensation temperature (T_c).

$$\dot{m}_m = B_1 + B_2 T_e + B_4 T_e^2 + B_7 T_e^3 + \left(B_3 + B_5 T_e + B_8 T_e^2\right) T_c + \left(B_6 + B_9 T_e\right) T_c^2 + B_{10} T_c^3 \tag{1}$$

$$\dot{W}_{cp} = B_1 + B_2 T_e + B_4 T_e^2 + B_7 T_e^3 + \left(B_3 + B_5 T_e + B_8 T_e^2\right) T_c + \left(B_6 + B_9 T_e\right) T_c^2 + B_{10} T_c^3 \tag{2}$$

The coefficients of the Eq. 1 and 2 are listed in Tab. 1. To obtain the Eq. 1 the manufacturer performed test with a fixed temperature at the inlet of the compressor (35^{o}C). For lower evaporation temperature, this condition is not achieve in air conditioner. In order to correct the mass flow rate in the Eq. 1, AHRI (2005) suggest the Eq. 3 to evaluate the refrigerant

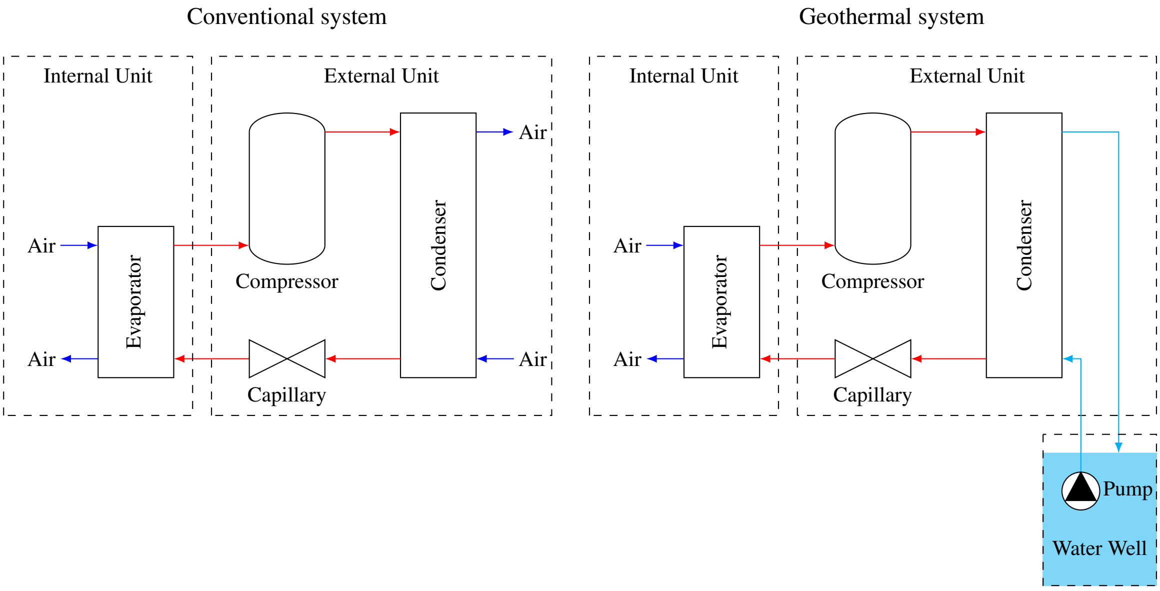

Figure 1. Main components of conventional and geothermal air conditioner system.

corrected mass flow rate ($\dot{m}_r$). AHRI (2005) comment that the variation on super-heating has negligible effects in power consumption.

$$\dot{m}_r = \frac{\rho_1}{\rho_m}\dot{m}_m \tag{3}$$

In this equation, ρ_1 is the density at the inlet of the compressor, and ρ_m is the density calculated using the fixed temperature (35^{o}C) give by the manufacturer.

2.1.2 Capillary tube

The expansion device typically used in an air conditioner is the capillary tube. The correlation of Rasti and Jeong (2018) was chosen to calculate the mass flow rate in the capillary tube because yields good agreement with 1052 sets of experimental data produced from five different refrigerants, including the R410A. The mass flow in the capillary tube is calculated by:

$$\dot{m} = 150,26\Pi_a^{-0,5708}\Pi_b^{-1,4636}\Pi_c^{1,953}\Pi_d^{0,6436}\Pi_e^{0,14181}\Pi_f^{-0,0158}D_c\mu_f \tag{4}$$

where L_{cap} is the capillary tube length, D_c is the capillary tube inside diameter, $P_{c,in}$ is the capillary tube inlet pressure, μ_f is the capillary inlet saturated liquid viscosity, ν_f is the capillary inlet liquid saturated specific volume, μ_f is the capillary inlet saturated vapor specific volume, i_{fgc} is the latent heat of vaporization at capillary inlet pressure, i_f is satured liquid specific enthalpy at capillary inlet pressure, $i_{c,in}$ is the capillary inlet specific enthalpy and L_{coil} is the coiled capillary tube length. The equation 3 used to calculate the density at the inlet of the compressor, thence the superheating. The dimensionless parameters are shown in Tab. 2.

2.1.3 Heat exchangers

The evaporator and condenser are modeled using the effectiveness-NTU method as made by Rabelo *et al.* (2019). The balance of energy in the refrigerant and air in the heat exchangers are given by:

$$\dot{Q} = \dot{m}_r(i_o - i_i) = \dot{m}_a C_{pa}(T_i - T_o) \tag{5}$$

Table 1. Parameters of the equations of the compressor

	B_1	B_2	B_3	B_5	B_5
$\dot{m}_m$	1.975964E-2	-9.623655E-5	-1.159600E-4	-8.356414E-6	2.575877E-5
$\dot{W}_{cp}$	1.485628E+2	-9.748167E+0	2.360980E+1	-1.372568E+0	4.168670E-01
	B_6	B_7	B_8	B_9	B_{10}
$\dot{m}_m$	-1.557530E-6	6.290759E-8	5.195857E-7	-3.186213E-7	2.287479E-8
$\dot{W}_{cp}$	-3.283619E-1	4.620434E-2	4.604102E-3	-9.753143E-4	2.993434E-3

Table 2. Dimensionless Parameters

Parameter	Definition	Description
Π_a	L_{cap}/D_c	Effect of capillary tube total length and inside diamenter
Π_b	$D_c^2 i_{fgc}/\nu_f^2 \mu_f^2$	Effect of the latent heat of vaporization
Π_c	$D_c^2 P_{c,in}/\nu_f \mu_f^2$	Effect of the capillary tube inlet pressure
Π_d	$1 + (i_{c,in} - i_f)/i_{fg}$	Effect of enthalpy at the capillary tube inlet
Π_e	ν_g/ν_f	Effect of the density
Π_f	$1 + L_{coil}/d_{coil}$	Effect of the coiled capillary tube length and coil diameter

where $\dot{Q}$ is the heat transfer rate, i is the refrigerant specific entalphy, $\dot{m}_a$ is the air mass flow rate, C_{pa} is the air heat capacity at constant pressure and T is the air temperature. The subscripts i and o refers to inlet and outlet of the heat exchanger. In the water-cooled condenser, the properties of air are replaced by properties of water. The maximum heat transfer rate calculate by:

$$\dot{Q}_{max} = \dot{C}_{min}(T_{hi} - T_{ci}) \tag{6}$$

where $\dot{C}_{min}$ is the smaller heat capacity rate, T_{hi} is inlet temperature of hot fluid and T_{ci} is inlet temperature of cold fluid. The heat capacity rate and refrigerant heat capacity at constant pressure (C_{pr}) can be expressed as:

$$\dot{C} = C_p \dot{m} \tag{7}$$

$$C_{pr} = \frac{i_i - i_o}{T_i - T_o} \tag{8}$$

The effectiveness (ε) of heat exchanger is evaluated as follows Incropera *et al.* (2007):

$$\varepsilon = \frac{\dot{Q}}{\dot{Q}_{max}} \tag{9}$$

The effectiveness can also be expressed by Eq. 10 for cross-flow, single-pass, both fluids unmixed and by Eq. 11 for double pipe counter-flow heat exchanger (ASHRAE (2013)).

$$\varepsilon = 1 - \exp\left[\left(\frac{\dot{C}_{max}}{\dot{C}_{min}}\right)\text{NTU}^{0.22}\left\{\exp\left[-\left(\frac{\dot{C}_{min}}{\dot{C}_{max}}\right)\text{NTU}^{0.78}\right] - 1\right\}\right] \tag{10}$$

$$\varepsilon = \frac{1 - \exp[-\text{NTU}(1 - \dot{C}_{min}/\dot{C}_{max})]}{1 - \exp[-\text{NTU}(1 - \dot{C}_{min}/\dot{C}_{max})]\dot{C}_{min}/\dot{C}_{max}} \tag{11}$$

In these equation NTU is number of transfer units and is expressed as:

$$\text{NTU} = \frac{UA}{\dot{C}_{min}} \tag{12}$$

where A is the heat transfer surface area of the heat exchanger and U is the overall heat transfer coefficient given by:

$$U = \left(\frac{1}{\bar{h}_a} + \frac{1}{\bar{h}_r}\right)^{-1} \tag{13}$$

the mean refrigerant heat transfer coefficient ($\bar{h}_r$) is calculated integrating numerically in function of specific entalphy as made by Zhang *et al.* (2014). In the condenser the correlation of Gnielinski (1976) is used if $i \geq i_V$ or $i \leq i_L$ and the correlation of Shah (2016) is used if $i_L < i < i_V$. In the evaporator the correlation of Gnielinski (1976) is used if $i \geq i_V$ and the correlation of Shah (2017) is used if $i_L < i < i_V$. To evaluate the mean air heat transfer coefficient ($\bar{h}_a$), Incropera *et al.* (2007) suggest the correlation of Grimson (1937), that it is given by:

$$\bar{h}_a = B_0 Re_{max}^m Pr^{1/3}(k/D) \tag{14}$$

where the k is the thermal conductivity, D is external diameters of the tube and Pr is the Prandtl number. The coefficients B_0 and m are listed for aligned or staggered tubes and for different transverse pitch and longitudinal pitch. In this work, due the geometry of the heat exchangers the B_0 coefficient is 0.4545764 for the condenser, 0.38307 for the evaporator and the m coefficient is 0.568 for both heat exchanger. The Re_{max}, for the specific geometry of heat exchanger used in this work, is given by:

$$Re_{max} = \frac{2\rho VD}{\mu} \tag{15}$$

where V is the air velocity at the inlet of evaporator and μ is the viscosity. In the water-cooled condenser, air heat transfer coefficient are replaced water heat transfer coefficient in the Eq. 13. The mean water HTC ($\bar{h}_w$) is calculated using the correlations described by Rohsenow *et al.* (1998) for flow in annular regions.

In fact the pressure of the refrigerant is not known and not appear in non of the equations present. Therefore a value for the pressure of the refrigerant is estimated and an error is calculated comparing the effectiveness of Eq. 9 and 10 and secant method describe by Chapra and Canale (2008) is used to find a pressure that gives an error lower than 0.1%. For the water-cooled condenser, the error is calculated comparing the effectiveness of Eq. 9 and 11.

The balance of energy in the air in the evaporator is evaluated from EQ. 16 to compute the condensation of water present in the air.

$$\dot{Q}_e = \dot{m}_a C_p (T_o - T_i) + \dot{m}_{ce} i_{fg} \tag{16}$$

where $\dot{m}_{ce}$ is the mass flow rate of condensation water in the evaporator. The data of heat exchangers are listed in Tab. 3.

2.1.4 Pump

The electric power consumption in the pump ($\dot{W}_p$), evaluated as follow:

$$\dot{W}_p = \frac{\dot{m}_w}{\rho_w \eta_p} \sum \Delta P_f \tag{17}$$

where η_p is the pump overall efficiency and ΔP_f is the friction loss. At each stretch of piping the friction loss is evaluated by Eq. 18. To calculate the Darcy friction factor (f) was used the correlation of Churchill (1977) for flow in circular ducts, the correlation of Natarajan and Lakshmana (1973) for laminar flow in annular ducts and Jones and Leung (1981) for turbulent flow in annular ducts.

$$\Delta P_f = \frac{8 f L \dot{m}_w^2}{\pi^2 D_i^5 \rho_w} \tag{18}$$

The pump selected for this work is manufactured by Dancor model DS4. The pump head (H) and overall efficiency (η_p) is given by EQ. 19 and 20, that were adjusted using the data from manufactured catalog. The mass flow of the pump is calculate equalling the losses in Eq. 18 to the head in Eq. 19.

$$H = 2.1739\dot{m}_w^2 - 1.0519\dot{m}_w + 6 \tag{19}$$

$$\eta_p = 1.0319\dot{m}_w - 0.7023\dot{m}_w^2 \tag{20}$$

2.2 Refrigerant charge

Another important parameter in the cost of the system is the refrigerant charge. The required mass of the refrigerant (m) is evaluated by the Eq. 21 for single phase flow and by the Eq. 22 for two phase flow.

$$m = \int \rho dV \tag{21}$$

$$m = \int \left[\alpha \rho_v + (1-\alpha)\rho_l\right] dV \tag{22}$$

where the subscripts l and v refers to the liquid and to the vapor, respectively, and the void fraction (α) is calculated by Hughmark (1965) correlation. The equation 21 and 22 are integrated numerically with constant specific entalphy step as made by Zhang *et al.* (2014) and Duarte (2018). To evaluate the charge of refrigerant the piping between the internal and external unit was considered 7m long and piping between components inside the external unit 0,3m long.

2.3 Thermal zone mathematical model

To compare the performance of the geothermal air conditioner with a convectional air-to-air system, an office cooling was chosen as application. The office chosen has length of 3m, width of 3m and wall height of 2.8m that is occupied from Monday to Friday and from 8 am to 6 pm. The power generate ($\dot{Q}_g$) inside the office is given by:

$$\dot{Q}_g = N_p F_p + \dot{Q}_{eq} \tag{23}$$

where N_p is the number of people, F_P the power generation per person factor, A_f in the ceiling or floor area and $\dot{Q}_{eq}$ the power generation by electrical equipment. F_P and $\dot{Q}_{eq}$ is listed in ABNT (2008) for different applications and equipment, the values selected are 130W/person and 720W. The power generation by electrical equipment take account computers, printers and lighting. The heat transfer rate through the wrapper ($\dot{Q}_{wr}$) (walls, floor and ceiling) is evaluated by:

$$\dot{Q}_{wr} = UA(T_{ex} - T_{in}) \tag{24}$$

where A is area of heat transfer, T_{ex} is the external temperature and T_{in} is the internal temperature. The values of overall heat transfer U listed by ABNT (2005b,c) different materials and constructive system typically used in Brazil and the values used are listed in Tab. 3. The ABNT (2005b) suggest the EQ. 25 to evaluate heat gain due solar radiation.

$$\dot{Q}_{sol} = 0.04UA\alpha I \tag{25}$$

In this equation α is the solar absorptivity and I is the solar radiation. ABNT (2005b,c) presents values for solar absorptivity and thermal delay (ϕ). The thermal delay is defined by ABNT (2005a) as time elapsed between a thermal variation in a medium and its manifestation on the opposite surface of a constructive component subjected to a periodic regime of heat transmission. Therefor the solar radiation used in Eq. is evaluate at time $t = t - \phi$. Finally, the variation of internal temperature in given by:

$$T_{in} - T_{in}^0 = \frac{\Delta t}{C_{in}}(\dot{Q}_g + \dot{Q}_{sol} + \dot{Q}_{wr} - \dot{Q}_e) \tag{26}$$

where T_{in}^0 is the internal temperature evaluated at time $t = t - \Delta t$ and C_{in} thermal capacitance of the internal ambient. The value of thermal capacitance used is 750kJ/K that was estimate take account desks, chairs, computers, printers, air, evaporator unit, cabinet, paper, etc. The terms in the right of Eq. 26 were calculate at using T_{in}^0. In this work was used a dynamic time step, Δt. The time step was calculate for maximum internal temperature variation of 0.5^{o}C as long as it was within range of 5 and 60 minutes.

2.4 Performance indicators

The coefficient of performance (COP) is defined as follow:

$$COP = \frac{\dot{Q}_e}{\dot{W}_{cp} + \dot{W}_e + \dot{W}_{cd}} \tag{27}$$

where $\dot{W}_e$ is the power consumed by the evaporator fan and $\dot{W}_{cd}$ is the power consumed by the condenser fan or pump. The air mass flow rate and fan power were assumed constant.

The payback period ($\hat{P}$) of the geothermal air conditioner over an conventional air conditioner, in years, if ($\hat{P}$) is higher than one year, is given by:

$$\hat{P} = \frac{\hat{I}}{\hat{S}(1 + \text{IR})^{(\hat{P}-1)}} \tag{28}$$

where $\hat{I}$ is the difference of initial investment between geothermal air conditioner over an conventional air conditioner, IR is the annual inflation rate and the annual savings ($\hat{S}$). The mean inflation rate of electricity in Brazil is 10% (Santos *et al.*, 2018). The annual savings is given by:

$$\hat{S} = \hat{E}_t(E_C - E_G) \tag{29}$$

Table 3. Main simulation parameters

Parameter	Value	Parameter	Value	Parameter	Value
Atmospheric Pressure	92 kPa	Evaporator fan power	33W	Evaporator fan power	45W
Capillary internal diameter	0.064 in	Evaporator fan mass flow	500kg/h	Condenser fan mass flow	1100kg/h
Capillary length	1.5m	Evaporator tube length	18 m	Condenser tube length	25 m
Capillary coil diameter	50mm	Evaporator heat transfer area	3.36m^2	Condenser heat transfer area	5.08 m^2
Electricity tariff	0.95 R$/kWh	Evaporator frontal area	775cm^2	Condenser frontal area	876 cm^2
Wall overall heat transfer	2.58 W/(m^{2}K)	Moisture removal	1kg/h	Condenser pipe diameter	5/16 in
Floor overall heat transfer	1.59 W/(m^{2}K)	Number of people	4	Water PVC piper diameter	20mm
Ceiling overall heat transfer	1.92 W/(m^{2}K)	Ceiling thermal delay	3.6 h	Ceiling solar absorptivity	0.3
Refrigerant charge	0.535kg	Water well depth	20m	Water well temperature	22^{o}C
AC Conventional	1800R$	AC Geothermal	6200R$	Water well cost	200R$/m

where $\hat{E}_t$ is the electricity tariff, E_C is annual electrical energy consumed by conventional system, E_G is annual electrical energy consumed by geothermal system. A list of the parameters used in the following simulations is presented in Tab. 3. The costs in Tab. 3 are based in the Belo Horizonte market in March of 2020.

3. RESULTS

To compare the performance of a convectional air conditioner and a geothermal air conditioner, the hourly climate data recorded in the Pampulha (Belo Horizonte, MG) whether station were considered. The period between June of 2019 and May of 2020 was analyzed, and the day with highest temperatures was September 13, 2019. The solar radiation and air temperature obtained from INMET website for the mentioned whether station is shown in Fig. 2 for September 9 to 13, 2019. The office internal temperature and the air conditioner COP is also shown in Fig. 2 for both setup. This figure shown that COP of geothermal system is better, most of time, than convectional system.

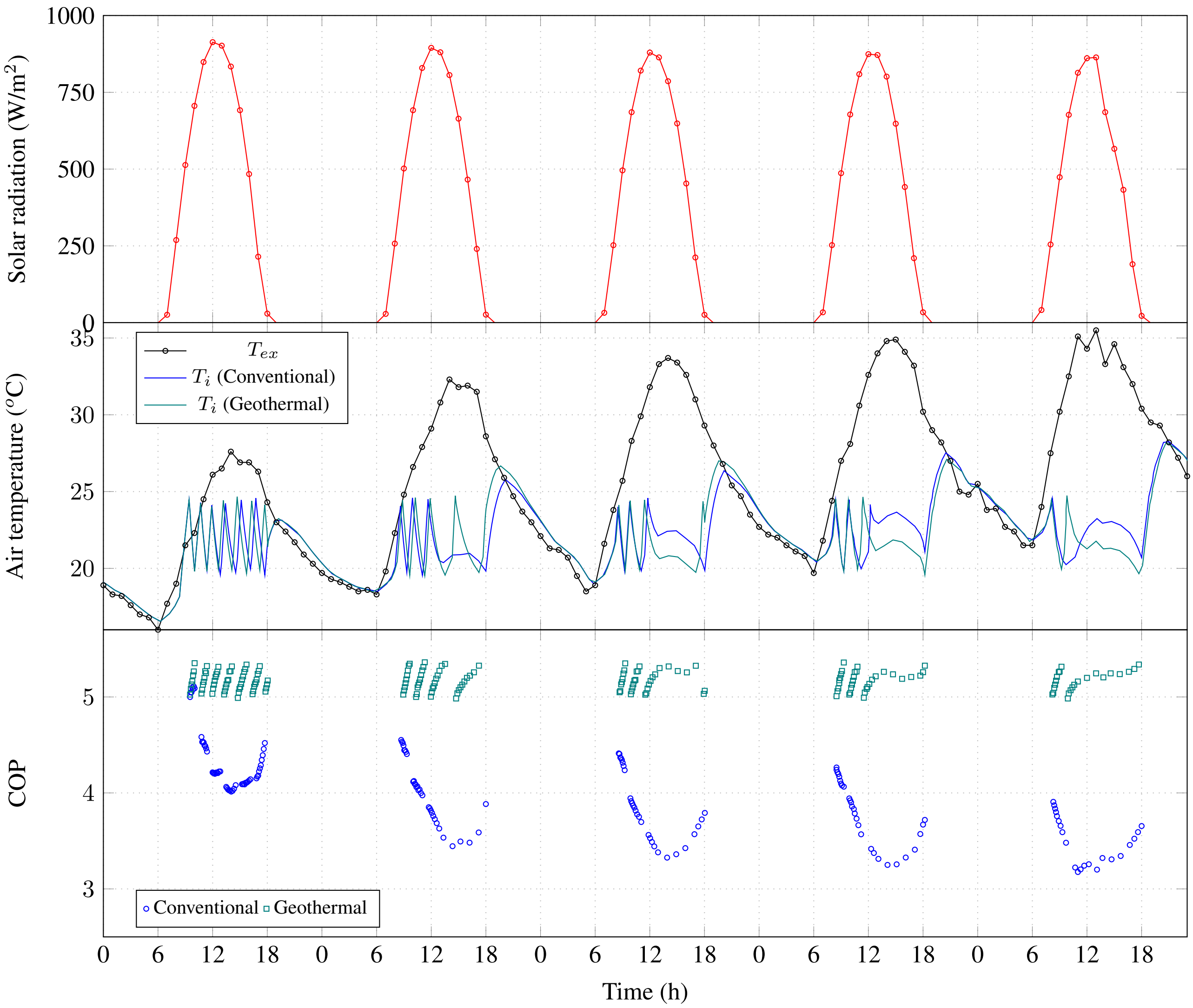

Figure 2. Solar radiation, temperatures and COP for September 9 to 13, 2019

The difference of the internal office temperature in Fig. 2 is justified by the variation in the cooling capacity. In the conventional system, if the external air temperature increases, the condensation temperatures also increases and reduces the COP and the cooling capacity. In the geothermal system, the water well temperature is constant, so the cooling capacity is not affected by external air temperature. The COP of geothermal system increase with the reduction of the internal air temperature for the range of 24 to 20^{o}C, in this range, the sub-cooling reduces and the superheating decreases lead to a higher COP. The same effects of sub-cooling and the superheating in COP also discussed by Belini (2019). This difference of cooling capacity associate with the ON/OFF control strategy, typically used in this application, lead to a lower time of operation that is 9% lower in geothermal AC in comparison with conventional AC.

The results of monthly and annual mean COP are presented in Fig. 3 and Tab. 4 considering the solar radiation and air

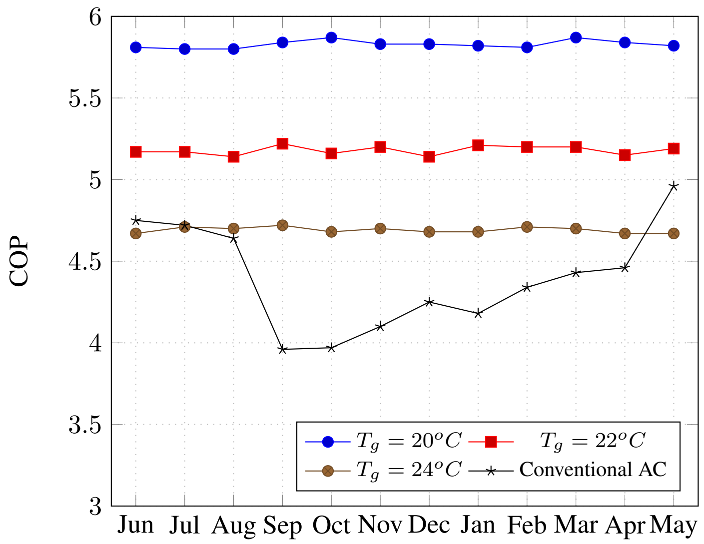

Figure 3. Caparison of monthly COP of the systems operating in Belo Horizonte between June of 2019 and may of 2020 and considering different ground water temperature (T_g).

temperature of Belo Horizonte in the period between June of 2019 and May of 2020. In these simulations was considered that the occupation of was not affected by the coronavirus pandemic. During the national and municipal holidays the office was considered empty. The ground water temperatures was chosen using as reference the results presented by Hamza *et al.* (2005), Souza Filho *et al.* (2013) and Dantas *et al.* (2017). The monthly COP of geothermal, for the results that used the water well temperatures of 20^{o}C and 22^{o}C, are better than the COP of conventional system for any month and for the water well temperatures of 24^{o}C only in 3 months the conventional system has batter COP. The geothermal annual COP, as listed in Tab. 4, are 33%, 18% and 6.8% better than the COP of conventional system, for the water well temperatures of 20, 22 and 24^{o}C, respectively. The geothermal annual energy consumption, as listed in Tab. 4, are 27%, 16% and 9.7% lower than the energy consumption of conventional system, considering the water well temperatures of 20, 22 and 24^{o}C, respectively.

In order to complement the energetic analyses above presented and economical analysis was made to verify the feasibility. As discussed by Duarte *et al.* (2019a) the water well depth is an important parameter in the economical analysis of a refrigeration system that uses geothermal energy. Four different water well depth (Z) was considered as listed in Tab. 4. In theory, a water well deeper should indicate a lower the COP due higher pressure drop in the pipes (EQ. 18) and consequently higher pumping energy consumption (EQ. 17). An sensitivity analysis was conducted to evaluate the influence of water well depth in the monthly COP. The reduction of water well depth from 20 to 0 meters increase the monthly COP only 0.02%, therefore the results are only presented to demonstrate the influence of water well depth in initial investment and consequentially in the payback. The payback period of the geothermal air conditioner over an conventional air conditioner are listed in Tab. 4. The results of payback in Tab. 4 are in the same range (9 to 16 years) of the payback founded by Kharseh *et al.* (2015) residential buildings using ground source heat pump systems in cooling-dominated environments. A similar result is presented by Duarte *et al.* (2019a) showing that the payback of the system is strongly affected by water well depth and lightly affected by by water well temperature.

Table 4. Annual results for the systems operating in Belo Horizonte between June of 2019 and may of 2020, considering different water well temperature (T_g) and depth (Z)

	$T_g = 20^oC$	$T_g = 22^oC$	$T_g = 24^oC$	Conventional AC
COP	5.83	5.18	4.69	4.39
Energy Consumption (kWh)	646.2	736.6	793.2	878.6
Payback (years) (Z=20m)	9.2	11.7	14.7	-
Payback (years) (Z=10m)	6.5	8.6	11.2	-
Payback (years) (Z=5m)	4.5	6.3	8.5	-
Payback (years) (Z=0m)	1.7	2.6	3.8	-

4. CONCLUSIONS

In this paper, an energetic and economic analysis of a R410A Geothermal air conditioner was carried out using a mathematical model. The system considered has an open loop ground underground (aquifer) water and was compared to conventional air-to-air air conditioner. To compare the performance of both system, an office cooling was used as application. The simulations was made considering the climate of Belo Horizonte, Brazil using weather data obtained from June of 2019 to May of 2020. The results show that the annual COP of Geothermal air conditioner are 33% to 6.8% better than conventional air conditioner depending on the water well temperature. The reduction of annual energy consumption were in range of 9.7% to 27%. The results of payback are in the same range of the payback reported in the literature for similar applications.

5. ACKNOWLEDGEMENTS

This work was supported by Foundation for Research Support of the State of Minas Gerais (FAPEMIG), National Council for Scientific and Technological Development (CNPq) and Coordination of Improvement of Higher Level Personnel (CAPES).

6. REFERENCES

ABNT, 2005a. *NBR15220-1: Desempenho Térmico de Edificações-Parte 1: Definições, símbolos e unidades*. Associação Brasileira de Normas Técnicas.

ABNT, 2005b. *NBR15220-2: Desempenho térmico de edificações Parte 2: Método de cálculo da transmitância térmica, da capacidade térmica, do atraso térmico e do fator solar de elementos e componentes de edificações*. Associação Brasileira de Normas Técnicas.

ABNT, 2005c. *NBR15220-3: Desempenho térmico de edificações Parte 3: Zoneamento bioclimático brasileiro e diretrizes construtivas para habitações unifamiliares de interesse social*. Associação Brasileira de Normas Técnicas.

ABNT, 2008. *NBR16401-1. Instalação de ar-condicionado-Sistemas centrais e unitários Parte 1: Projeto das instalações*. Associação Brasileira de Normas Técnicas.

AHRI, 2005. *CAN/ANSI/AHRI 540-2015, Performance Rating of Positive Displacement Refrigerant Compressors and Compressor Units*. Air Conditioning, Heating and Refrigeration Institute.

ASHRAE, 2013. *ASHRAE Handbook - Fundamentals (SI Edition)*. American Society of Heating, Refrigerating and Air-Conditioning Engineers, Inc. ISBN 978-1-936504-46-6.

Beckers, K.F., Aguirre, G.A. and Tester, J.W., 2018. "Hybrid ground-source heat pump systems for cooling-dominated applications: Experimental and numerical case-study of cooling for cellular tower shelters". *Energy Buildings*, Vol. 177, pp. 341–350.

Belini, R.J., 2019. "Avaliação de fatores que afetam a eficiência energética em um sistema de refrigeração". In *XVI CONBRAVA - Congresso brasileiro de refrigeração, ar condicionado, ventilação, aquecimento e tratamento do ar*.

Blázquez, C.S., Verda, V., Nieto, I.M., Martín, A.F. and González-Aguilera, D., 2020. "Analysis and optimization of the design parameters of a district groundwater heat pump system in turin, italy". *Renewable Energy*, Vol. 149, pp. 374 – 383. ISSN 0960-1481.

Chapra, S.C. and Canale, R.P., 2008. *Métodos numéricos para engenharia*. McGraw-Hill.

Churchill, S.W., 1977. "Friction-factor equation spans all fluid-flow regimes". *Chemical engineering*, Vol. 84, No. 24, pp. 91–92.

Dantas, D., Barbosa, G.P., Cunha, E.G.S., de Souza, M.J.H. and de Souza, C.M.P., 2017. "Temperatura do ar e do solo em diferentes profundidades, em diamantina-mg/air temperature and soil in different depths in diamantina-mg". *Caderno de Ciências Agrárias*, Vol. 9, No. 3, pp. 61–66.

de Paula, C.H., Duarte, W.M., Rocha, T.T.M., de Oliveira, R.N. and Maia, A.A.T., 2020. "Optimal design and environmental, energy and exergy analysis of a vapor compression refrigeration system using R290, R1234yf, and R744 as alternatives to replace R134a". *International Journal of Refrigeration*, Vol. 113, pp. 10 – 20. ISSN 0140-7007.

Duarte, W.M., 2018. *Numeric model of a direct expansion solar assisted heat pump water heater operating with low GWP refrigerants (R1234yf, R290, R600a and R744) for replacement of R134a*. Ph.D. thesis, UFMG.

Duarte, W.M., Paulino, T.F., Maia, A.A.T. and Machado, L., 2019a. "Feasibility of solar geothermal hybrid source heat pump for producing domestic hot water in brazilian climates". In *International Congress of Mechanical Engineering - COBEM 2019*. ABCM.

Duarte, W.M., Pabon, J.J.G., Maia, A.A.T. and Machado, L., 2019b. "Nonisentropic phenomenological model of a reciprocating compressor". *International Journal of Air-Conditioning and Refrigeration*, p. 1950039.

Duprez, M.E., Dumont, E. and Frère, M., 2007. "Modelling of reciprocating and scroll compressors". *International Journal of Refrigeration*, Vol. 30, No. 5, pp. 873–886.

EPE, 2018. *NOTA TÉCNICA EPE 030/2018. Uso de Ar Condicionado no Setor Residencial Brasileiro: Perspectivas e* *contribuições para o avanço em eficiência energética*. Ministério de Minas e Energia.

Gnielinski, V., 1976. "New equations for heat and mass transfer in turbulent pipe and channel flow". *Int. Chem. Eng.*, Vol. 16, No. 2, pp. 359–368.

Grimson, E.D., 1937. "Correlation and utilisation of new data on flow resistance and heat transfer for cross flow of gases over tube banks". *Trans. ASME.*, Vol. 59, pp. 583–594.

Hamza, V.M., Dias, F.J.S., Gomes, A.J. and Terceros, Z.G.D., 2005. "Numerical and functional representations of regional heat flow in south america". *Physics of the Earth and Planetary Interiors*, Vol. 152, No. 4, pp. 223 – 256. Thermally controlled processes and preserved thermal signatures within the Earth.

Hughmark, G., 1965. "Holdup and heat transfer in horizontal slug gas-liquid flow". *Chemical Engineering Science*, Vol. 20, No. 12, pp. 1007–1010.

Incropera, F.P., Lavine, A.S., Bergman, T.L. and DeWitt, D.P., 2007. *Fundamentos da Transferência do Calor e massa*. Editora LTC, 6th edition.

Jones, O.C. and Leung, J., 1981. "An improvement in the calculation of turbulent friction in smooth concentric annuli". *Journal of Fluids Engineering*, Vol. 103, No. 4, pp. 615–623.

Kharseh, M., Al-Khawaja, M. and Suleiman, M.T., 2015. "Potential of ground source heat pump systems in cooling-dominated environments: Residential buildings". *Geothermics*, Vol. 57, pp. 104–110.

Li, S.F., Liu, Z.h. and Wang, X.J., 2019. "A comprehensive review on positive cold energy storage technologies and applications in air conditioning with phase change materials". *Applied Energy*, Vol. 255, p. 113667.

Minetto, S., 2011. "Theoretical and experimental analysis of a CO_2 heat pump for domestic hot water". *International journal of refrigeration*, Vol. 34, No. 3, pp. 742–751.

Natarajan, N. and Lakshmana, S., 1973. "Laminar flow through annuli: analytical method of pressure drop". *Indian Chem. Eng*, Vol. 5, No. 3, pp. 50–53.

Ndiaye, D. and Bernier, M., 2010. "Dynamic model of a hermetic reciprocating compressor in on–off cycling operation". *Applied Thermal Engineering*, Vol. 30, No. 8, pp. 792–799.

Petit and Meyer, 1997. "A techno-economic analytical comparison of the performance of air-source and horizontal-ground-source air-conditioners in south africa". *International Journal of Energy Research*, Vol. 21, pp. 1011–1021.

PROCEL, 2008. *Pesquisa de posse de equipamentos e hábitos de uso: Setor comercial. Ano base: 2005.* PROCEL ELETROBRÁS.

Rabelo, S.N., Paulino, T.F., Machado, L. and Duarte, W.M., 2019. "Economic analysis and design optimization of a direct expansion solar assisted heat pump". *Solar Energy*, Vol. 188, pp. 164 – 174.

Rasti, M. and Jeong, J.H., 2018. "A generalized continuous empirical correlation for the refrigerant mass flow rate through adiabatic straight and helically coiled capillary tube". *Applied thermal Engineering*, Vol. 143, pp. 450–460.

Rohsenow, W.M., Hartnett, J.P., Cho, Y.I. *et al.*, 1998. *Handbook of heat transfer*, Vol. 3. McGraw-Hill, New York.

Santos, J.O., Cataldi, M., Herzog, M.M. and Pereira, E.M.D., 2018. "Comparação econômica entre o sistema de refrigeração fotovoltaico por compressão de vapor e chillers de absorção com coletores solares térmicos". In *CBENS 2018: VII Congresso Brasileiro de Energia Solar*. ABENS.

Shah, M.M., 2016. "Comprehensive correlations for heat transfer during condensation in conventional and mini/micro channels in all orientations". *International journal of refrigeration*, Vol. 67, pp. 22–41.

Shah, M.M., 2017. "Unified correlation for heat transfer during boiling in plain mini/micro and conventional channels". *International Journal of Refrigeration*, Vol. 74, pp. 604–624.

Souza Filho, M.N., Pereira, S.Y. and Barbuena, D., 2013. "Potencial geotérmico da bacia sedimentar de taubaté baseado em dados de perfilagem geofísica em poços–região leste do estado de são paulo". *Águas Subterrâneas*, Vol. 27, No. 1.

Tian, Q., Cai, D., Ren, L., Tang, W., Xie, Y., He, G. and Liu, F., 2015. "An experimental investigation of refrigerant mixture R32/R290 as drop-in replacement for hfc410a in household air conditioners". *International Journal of Refrigeration*, Vol. 57, pp. 216 – 228. ISSN 0140-7007.

Yu, Y., Li, H., Niu, F. and Yu, D., 2014. "Investigation of a coupled geothermal cooling system with earth tube and solar chimney". *Applied Energy*, Vol. 114, pp. 209–217.

Zhang, D., Wu, Q., Li, J. and Kong, X., 2014. "Effects of refrigerant charge and structural parameters on the performance of a direct-expansion solar-assisted heat pump system". *Applied Thermal Engineering*, Vol. 73, No. 1, pp. 522 – 528.

7. RESPONSIBILITY NOTICE

The authors are solely responsible for the printed material included in this paper.